JOURNAL OF CATALYSIS **159,** 383–393 (1996)
ARTICLE NO. 0101

Nitriles and Hydrogen on a Nickel Catalyst: Theoretical Evidence of a Process Competing with the Total Hydrogenation Reaction

Bernard Bigot, Françoise Delbecq, Anne Milet, and Vincent-Henri Peuch

Laboratoire de Chimie Théorique, Ecole Normale Supérieure de Lyon, 46, Allée d'Italie, 69364 Lyon Cedex 07, France; and Institut de Recherches sur la Catalyse, CNRS, LP 5401, 2, Avenue Albert Einstein, 69626 Villeurbanne Cedex, France

Received May 24, 1995; revised November 21, 1995; accepted November 30, 1995

Possible reaction steps occurring when nitriles and hydrogen are simultaneously adsorbed on nickel have been investigated by means of semi-empirical extended Hückel calculations. The study of the reactivity has been carried out on Ni(100): after the first hydrogenation step which principally yields imido-ethylidene ($CH_3CH{=}N{-}$), both adsorbed perpendicular and parallel to the metallic surface, we predict a competition between a second hydrogenation, which leads to a nitrene species ($CH_3CH_2{-}N{=}$) doubly bonded to the surface, and a coupling process involving a C–C bond formation. For each of these steps, activation energies have been estimated, and the stabilities of the a priori possible adsorbed forms of the intermediates have been compared.

I. INTRODUCTION

The existence of by-products to the hydrogenation of nitriles of fatty acids on a nickel catalyst has costly consequences on many major industrial syntheses. This is especially true with the hydrogenation of adiponitrile into hexamethylenediamine, which is one of the two major reactants used in the industrial synthesis of Nylon 6-6. This hydrogenation also yields a very small amount (ppm) of cyclized products, secondary and tertiary amines. Even though such small quantities do not make a separation process worthwhile, the presence of these reactants as possible candidates for the polycondensation results in a weakening of the Nylon threads. Our aim is to understand what regulates the competing processes when hydrogen and nitriles are simultaneously adsorbed on nickel.

In a previous paper (1), we have studied the adsorption of acetonitrile on three selected faces of nickel [(111), (100), and (110)] by means of extended Hückel calculations. We have concluded on the most favorable mode on each face for this molecule, taken as a model for aliphatic nitriles. The face for strongest adsorption appears to be the (110), where acetonitrile is preferentially adsorbed parallel to the surface (η_2), with both nitrogen and carbon atoms linked to the metal ($E_{\text{adsorption}} = 1.74$ eV); on (100) also, the stablest geometry is η_2 with $E_{\text{adsorption}} = 1.52$ eV; lastly, on (111) we conclude to the existence of a possible competition between η_2 and η_1 forms (the latter with CN perpendicular to the surface, $E_{\text{adsorption}}$ in the 1.13–1.39 eV range). The geometries we predict and the relative stabilities we find are in fair agreement with the available experimental data. The interpretation, based on the analysis of density of state (DOS) and of crystal orbital overlap population (COOP) curves, highlights the competition between the two-electron stabilizing effects and the destabilizing four-electron ones (2, 3). The careful study of the adsorbed forms of acetonitrile shows unsurprisingly that the greater the bonding with the surface, the weaker the C–N bond and therefore the more reactive the nitrile.

Although already extensively documented, both at a theoretical level (4–8) and at an experimental one (9, 10), the adsorption of atomic hydrogen on Ni(100), Ni(110), and Ni(111) has been investigated in order to build a consistent basis to the study of the coadsorption of acetonitrile and atomic hydrogen on the one hand, and of the further steps of hydrogenation on the other hand. Ni(110) is subject to surface reconstructions (9, 10) and finely divided catalysts principally exhibit (100) and (111) faces (11, 12). This led us to focus on Ni(100) for the study of the reactivity. The similar study on Ni(111) is under progress and will be published later.

Two possible first hydrogenation intermediates have been experimentally observed: imido-ethylidene ($-N{=}CHCH_3$), η_1 and η_2 adsorbed (13–16), and imino-ethyl ($HN{=}C(CH_3){-}$), mostly η_2 adsorbed (17, 18). An interesting point is raised by the possibility of the synthesis of vicinal diamine via N-metal imines (19), showing a radical reactivity of carbon in imidoethylidene; this could, in our case, indicate a possible coupling of two CN, by C–C bond formation. This study aims at providing a theoretical support to these observations and at further completing them.

II. METHODOLOGY

All the adsorptions and coadsorptions, both of the final products as well as of the several possible intermediates,

0021-9517/96 $18.00

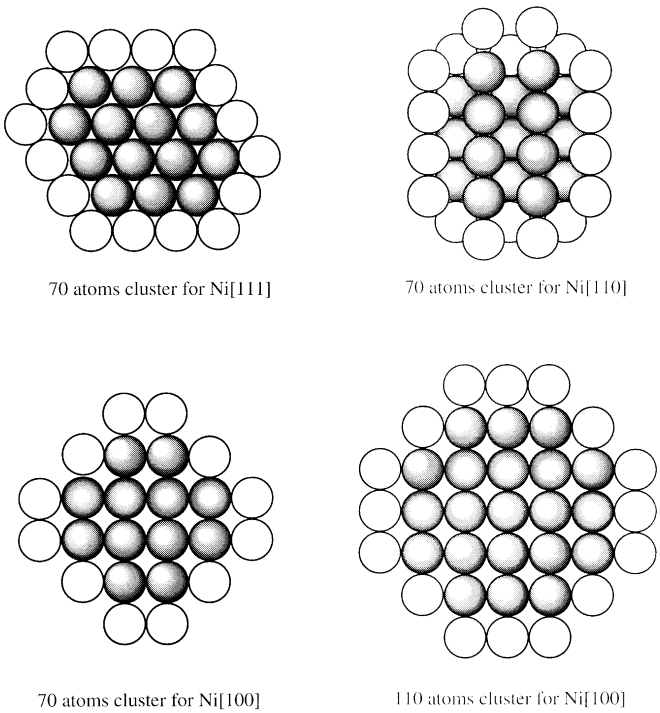

FIG. 1. Top view of the different metallic clusters used for the calculations. Surface core atoms are shaded.

have been studied with the same semi-empirical extended Hückel (EH) method. This technique models an extended metallic surface by a large (70 to 110 atoms) cluster divided into a core part, on which adsorption takes place, and an outer shell, necessary to provide the core atoms with realistic electronic characteristics (2, 3). The clusters we have used are presented in Fig. 1. It has been checked that the electronic characteristics of the core atoms of these clusters are consistent. All the reaction steps we have considered involved adsorbed intermediates on unreconstructed faces.

As in Ref. (1), distances between chemically linked atoms are fixed at values making sense with the distances experimentally observed in a variety of organometallic complexes (C=N, 1.30 Å; C–N, 1.47 Å; N–H, 1.05 Å; Ni–H, 1.80 Å). The EH method does not allow any optimization of the parameters and the quantitative values obtained should not be compared to the experimental values without special attention. Much in the same way, the atomic levels are fixed to values consistent with the previous systems already satisfactorily studied in our group (1–3), and which lead to realistic electron transfers. We mainly focus on giving insight on the most probable reaction steps and on the hierarchy between the possible adsorbed intermediates.

Each step of the hydrogenation process has been studied in the same way: first, the geometries in the adsorbed state of a large number of a priori possible reactants and products are separately examined; the few most probable beginning and final situations are selected. In each case, a linear parameter h is introduced, $h = 0$ corresponding to the beginning and $h = 1$ to the end. All geometrical parameters are varied linearly with h, hence bond formations and induced hybridization are simultaneously treated. A global activation energy can be estimated for each possible reaction path, on the basis of which conclusions can be drawn. The most probable final intermediate of each step is also further examined by means of COOP in order to analyze both its stability and its reactivity.

III. ADSORPTION OF ATOMIC HYDROGEN

Table 1 presents the main computed results for atomic hydrogen adsorption on Ni(100), Ni(110), and Ni(111). The several adsorption sites taken into account are depicted in Fig. 2. ΔE is the adsorption energy, which we take as the difference between the total energy of the cluster with one hydrogen adsorbed on the one hand, and the sum of the energy of the bare cluster and of atomic hydrogen on the other hand.

It arises that atomic hydrogen preferentially adsorbs on Ni(100), while its stability on Ni(110) is greater than on Ni(111). In good agreement with the previous experimental and theoretical studies (4–10), this is consistent with our result that atomic hydrogen favorably sits in the highest metallic coordination sites and that the stability directly increases

TABLE 1

Characteristics of Atomic Hydrogen Adsorption on Ni(100), Ni(110), and Ni(111)

Face	Site type	Sites[a]	ΔE (eV)	Hydrogen charge	Total surface/adsorbate overlap
100	Hollow	1,2,3	3.77	−0.31	0.608
	Bridge	4,5,6	3.45	−0.49	0.483
	On top	7,8	3.07	−0.66	0.331
110	Hollow	1,2,3,4	3.60	−0.39	0.570
	Bridge	7,8	3.46	−0.50	0.488
	Long bridge	11	3.55	−0.39	0.281
	On top[b]	5,6	3.20	−0.66	0.341
	On top[c]	9,10	3.14	−0.47	0.470
111	Hollow	1,2,3,4,5,6	3.50	−0.40	0.564
	Bridge	10,11	3.27	−0.48	0.466
	On top	7,8,9	2.96	−0.64	0.334

[a] EH calculations were performed on several sites of the same kind in order to check the homogeneity of the clusters. The numbers refer to Figs. 2a for face [100], 2b for face [110], and 2c for face [111]. Excellent coincidence of the results was obtained in each case.

[b] This is a real on top situation on a nickel atom of the above row.

[c] This is not a real on top adsorption; while being on top of a nickel atom of the underlaying row, the hydrogen atom has also nonnegligible interactions with four nickel atoms of above rows.

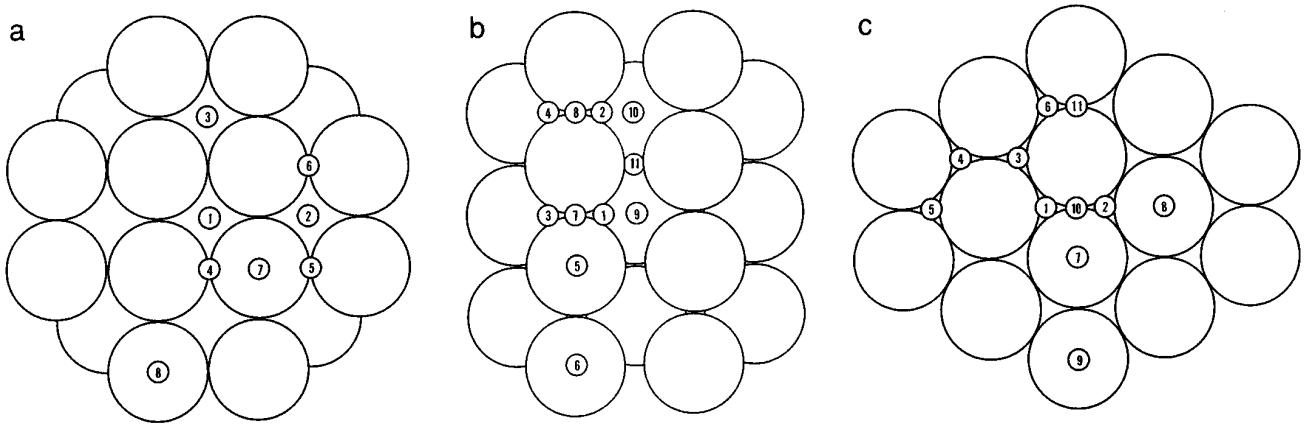

FIG. 2. Sites for atomic hydrogen adsorption on (a) Ni(100), (b) Ni(110), and (c) Ni(111). Only the surface nickel atoms of the core are drawn.

with the total adsorbate/surface overlap population. This means that the stabilizing two-electron interactions play a more important role than the destabilizing ones, illustrating with a simpler adsorbate the characteristic of nickel we had already observed with acetonitrile (1). We attribute this to the remarkably narrow *d* band of nickel among the transition metals. The differences between the faces are essentially due to the differences in coordination; the top and bridge absorptions are identical whatever the faces, while the hollow site on Ni(100), which involves four nickel atoms, is different from those on Ni(111) and Ni(110), which involve only three nickel atoms (see Fig. 2). Consequently, the characteristics of the top and bridge modes are the same on the three faces, while the hollow mode is stabler on Ni(100) than on the two other faces. We confirm the nature of the hydrogen–metal interaction: both the *s* and $d(d_{z^2}$ and, for the multi-coordinated sites, the adequate combinations of d_{xz} and d_{yz}) energy levels of nickel are involved. Thus we expect that any new adsorption of hydrogen or of any organic fragment or molecule in the vicinity will result in a destabilization on the hydrogen (see below), since they will compete for the same metallic orbitals.

Considering now the charge on the adsorbed hydrogen, we come to an interesting point which has already been raised by experimentalists (20). In all of the cases, hydrogen is negatively charged, consistent with the hydride reactivity often invoked for hydrogen adsorbed on nickel. The more the hydrogen is strongly bound to the surface, the less the charge transfer which occurs. This can be easily understood on the basis that increased overlap with the surface enables increased donation; hence the trend observed. This effect is pronounced since top hydrogen is twice as charged as hollow hydrogen and it will be notably more reactive than hollow and bridge hydrogen. This means the stablest adsorbed forms are not necessarily the ones involved in the successive steps of the reaction, a point we had constantly in mind for this study.

The values for hydrogen adsorption we present here are significantly larger than the experimental ones. Kristmann and co-workers (9) report values of 2.7 to 2.9 eV for such systems. However, their values are for coverages around one. Since we do not use any periodic boundary conditions with our model, the systems we have considered are equivalent to one atom of hydrogen adsorbed on an infinite plane. We have performed a few additional calculations with more than one hydrogen atom on the Ni(111) cluster. For coverage of unity (half of the hollow sites occupied) the adsorption energy we find decreases by 0.1 eV, while for higher coverages (up to two) we obtain an average 2.76 eV of adsorption energy per atom. However crude the EH method is, and even though it overestimates the binding energies (especially at low coverage), the result concerning the compared stabilities of the adsorption sites is correct. Our result is confirmed by density functional calculations (21).

IV. ACETONITRILE AND HYDROGEN COADSORPTION

Since we are studying the possibilities for an adsorbed phase reaction between acetonitrile and hydrogen, we have studied several cases of vicinal coadsorption on Ni(100), Ni(110), and Ni(111). The main characteristics of the situations we have considered are reported in Table 2 and the geometries are depicted in Fig. 3. In each case, only the stablest forms of acetonitrile have been considered, since we have already noted that the stronger the adsorption, the greater the effect on the CN bond and the more reactive the nitrile (1). On Ni(100) we have considered the η_2 fourfold (Fig. 3a) and two η_1 modes, hollow (Fig. 3b) and bridge (Fig. 3c); on Ni(111), the η_1 hollow mode (Fig. 3e) and the η_2 fourfold (Fig. 3d); and on Ni(110), only the stablest η_1 hollow mode. In contrast, we have considered in each case several positions (Greek letters) for the hydrogen atom since we have just seen the hydride reactivity of

TABLE 2

Coadsorption of Acetonitrile and Hydrogn on Ni(100), Ni(111), and Ni(110)

Acetonitrile	Hydrogen	Figure	Distance N–H (Å)	Distance C–H (Å)	C–N total overlap population	ΔE (eV)	Global effect (eV)
(100)	Hollow	3a, α	3.40	2.24	1.08	−1.13	0.38
η_2 fourfold		3a, β	1.96	3.13	1.11	−0.70	0.81
	Bridge	3a, γ	2.10	3.22	1.12	−0.90	0.61
(100)	Hollow	3b, α	2.51	2.90	1.55	−1.03	0.17
η_1 hollow	Bridge	3b, β	2.84	2.84	1.55	−1.12	0.08
(100)	Hollow	3c, α	2.98	3.56	1.63	−1.36	0.00
η_1 bridge	Bridge	3c, β	2.49	2.80	1.64	−1.21	0.15
(111)	Hollow	3d, α	4.10	2.81	1.08	−0.88	0.16
η_2 fourfold	Bridge	3d, β	2.54	2.62	1.08	−0.81	0.23
(111)	Bridge	3e, α	1.90	2.19	1.61	−1.39	0.01
η_1 hollow	On top	3e, β	1.54	1.55	1.76	−1.40	0.00
(110)	Hollow	3f, α	2.52	3.36	1.57	−1.14	0.28
η_1 hollow		3f, β	2.49	2.81	1.57	−1.23	0.21
	Bridge	3f, γ	2.39	2.47	1.57	−1.13	0.30
	On Top	3f, δ	2.41	2.90	1.57	−1.01	0.41
	On top (subj.)	3f, ε	2.53	2.69	1.57	−1.22	0.20

hydrogen was highly affected by the adsorption mode. Only the most favorable situations are reported in the table.

Two kinds of energies are reported in Table 2. One, noted ΔE, corresponds to the difference between the total energy of the system considered on the one hand, and to the sum of the energy of the corresponding hydrogenated cluster and of free acetonitrile on the other hand. Hence, it represents the binding energy of acetonitrile on a hydrogenated cluster. The other, noted as "global effect" in the table, represents the effect of the addition of the hydrogen atom on the adsorption of acetonitrile: it is the difference between ΔE and the adsorption energy of acetonitrile alone (see Introduction). The first observation is that many situations lead to negative ΔE, showing that a spontaneous coadsorption of acetonitrile and atomic hydrogen is possible. The second is that, in most cases, hydrogen tends to weaken acetonitrile adsorption as shown by positive values of "global effect". This last point has been experimentally observed (22). However, some of the situations are interesting as far as the H–nitrile bond formation is concerned. In all situations where the hydrogen is near enough, the C–H overlap population is always larger than the N–H one, indicating a tendency for H to stick on carbon.

If we take carbon–nitrogen total overlap population as an indicator of the reactivity of CN, we see that this characteristic is directly related to the adsorption mode, independently of the face. η_1 hollow modes yield a C–N overlap in the 1.40 to 1.60 range, η_1 bridge around 1.65, and η_2 fourfold in the 1.00 to 1.10 range. According to this, the η_2 fourfold mode appears to be the best form for reaction with hydrogen. We have focused the rest of the study on Ni(100), where the situations 3a(α), 3a(β) and, to a less extent since hydrogen is more distant, 3a(γ) seem to be the most favorable since an interaction occurs and mutual destabilization is not too important.

V. FIRST HYDROGENATION

There are two possible first hydrogenation intermediates of acetonitrile: either hydrogen bonds to the nitrogen of the nitrile or to the carbon. In the first case, the intermediate is an iminoethyl; in the second, it is an imido-ethylidene (see Scheme 1). Table 3 gathers the relative energies of the most probable adsorption modes of these two intermediates on Ni(100); zero energy has been attributed to the stablest of all modes. In each case, η_1 and η_2 coordinations have been considered and all the calculations have been performed using the 70 atoms cluster. As for acetonitrile in Ref. (1), a hybridization parameter has been introduced in the case of the η_2 absorptions, viz. 1 corresponding to full hybridization and 0 to no hybridization at all; bond distances and valence angles are varied simultaneously and linearly with this parameter. Again, we find that hybridization generally stabilizes the η_2 forms; we had attributed this to the fact that hybridization enhances the overlapping of the π orbitals of the adsorbate with the surface orbitals by providing a

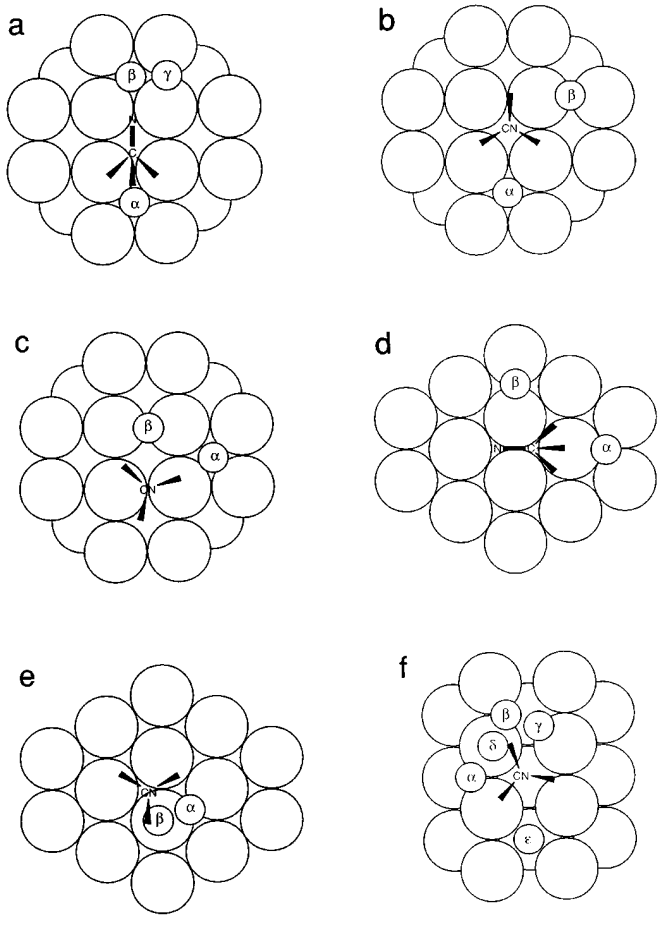

FIG. 3. Selected coadsorption geometries of acetonitrile and atomic hydrogen.

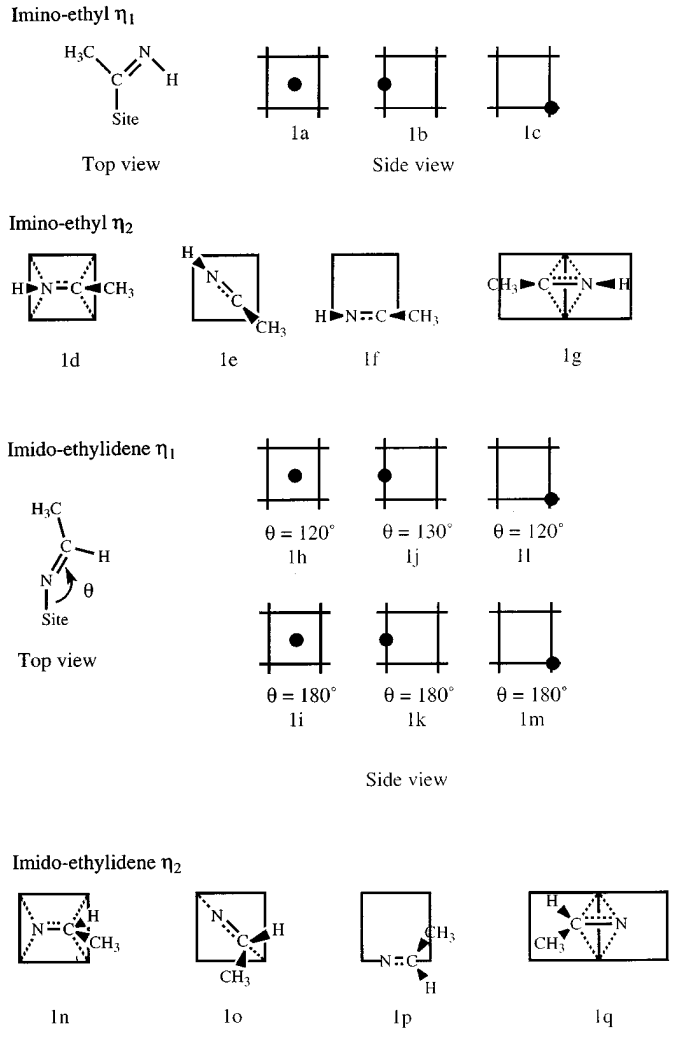

SCHEME 1. Adsorption geometries of the competitive first hydrogenation products of acetonitrile on Ni(100). See Table 3.

better interaction geometry and lowers the energy of the π^* orbitals. However, the hybridization of the π/π^* system of the C–N multiple bond requires a deformation energy, which balances the previous effect. The best value for the hybridization parameter for each η_2 form is also reported in Table 3.

It appears that the imido-ethylidene is far more stable than the imino-ethyl, even though the η_2 fourfold mode of this species reasonably competes with the best forms of the imido-ethylidene. The η_1 forms of the imino-ethyl are systematically destabilized (+2 eV) because of the steric hindrance of the methyl group with the surface. As far as the imido-ethylidene is concerned, the η_1 hollow adsorption is the stablest species with the N–C bond perpendicular to the surface.

Figure 4 shows the four possible competitive reaction steps which we have considered. The four energetic curves behave in a similar way: the starting points are all very close to equilibria, so the beginning is a destabilization; then, a positive overlap population either between C and H or between N and H appears and, as a bond is forming, the energy of the system decreases back. However, curve (1) presents two maxima: this is related to the fact that during its progression toward nickel, the hydrogen reaches a bridge position, which is a secondary minimum. If we compare the four energetic profiles, we find that (3) is undoubtedly the most favorable reaction path, for both the activation energy and the final energy are smaller than in the other cases. The activation energy we find in this case is below 1 eV, to be compared to more than 2 eV in the other cases. Our conclusion is that, as far as the first hydrogenation is concerned, hydrogen sticks to carbon and the most probable intermediate is an η_1 imido-ethylidene bound to the surface in a hollow site. This is consistent with the polarity of the CN bond in nitriles (1) compared to the hydride properties of adsorbed hydrogen. Moreover, work combining calculations and experiments (23, 24) has concluded on the same first-hydrogenation intermediate (imido-ethylidene) but by considering the reverse-path reaction. Since we find that the

TABLE 3

Adsorption Energies of the Competitive First Hydrogenation Products of Acetonitrile on Ni(100)

Intermediate type	Mode	Adsorption geometry (letters refer to Scheme 1)	Relative adsorption energy (eV)	Hybridization (η_2 modes)
Imino-ethyl η_1	Hollow	1a	2.20	
	Bridge	1b	1.74	
	Top	1c	2.29	
Imino-ethyl η_2	Fourfold	1d	0.36	1
	Di-σ diagonal	1e	2.01	0.7
	Di-σ	1f	1.84	0.7
	Di-σ $\perp$	1g	1.86	0.7
Imido-ethylidene η_1	Hollow	1h	0.10	
		1i	0.00	
	Bridge	1j	0.64	
		1k	0.51	
	Top	1l	1.08	
		1m	1.03	
Imido-ethylidene η_2	Fourfold	1n	0.41	1
	Di-σ diagonal	1o	1.03	0.7
	Di-σ	1p	0.91	0.7
	Di-σ $\perp$	1q	1.15	0.7

same species but η_2 bound to the surface in a fourfold site is very close energetically, it is possible to consider the coexistence of the two adsorption modes, which we kept as possible starting points for further reaction.

Regarding the reaction which follows, we have to define the description of the imido-ethylidene and to focus on the nature of the CN bond. The charge on nitrogen was -1.07 in the stablest nitrile form (η_2 fourfold) and is -0.66 in the stablest imido-ethylidene (η_1 fourfold); on carbon it was 0.38 to be compared to 0.55 in the intermediate. At the same time, the overlap population between carbon and nitrogen decreases from 1.12 to 1.05. It appears that the charge separation is less in the imido-ethylidene than in the nitrile (1.21 versus 1.45), showing a more pronounced radical character allowing a possible coupling process between two CN groups.

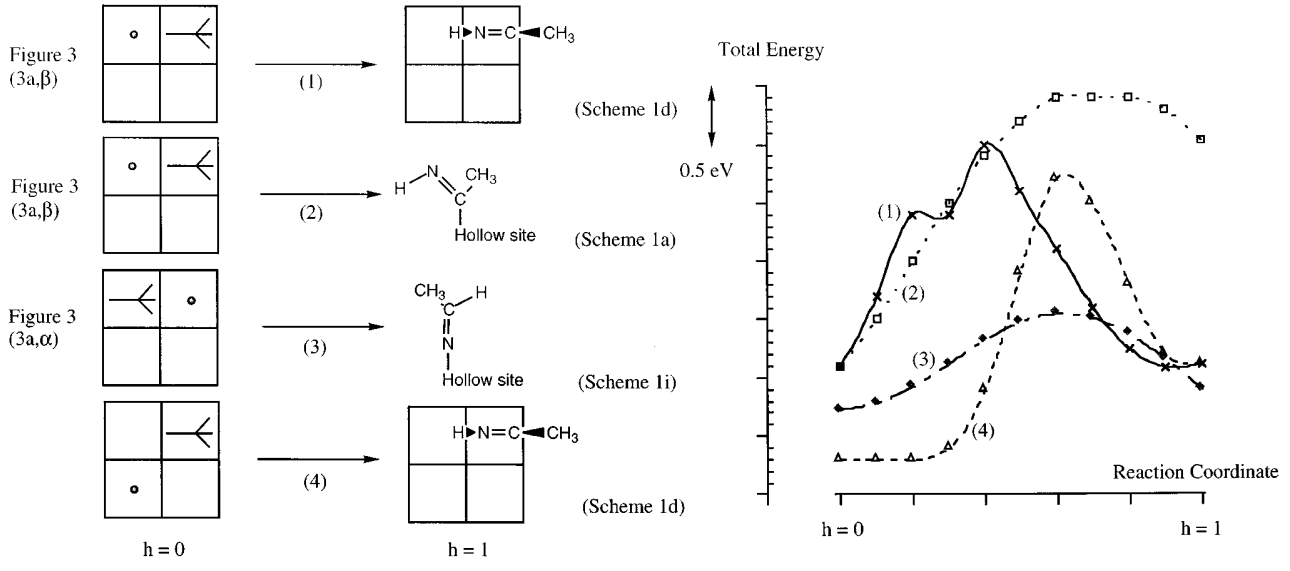

FIG. 4. Four of the most probable monohydrogenation steps of acetonitrile on Ni(100). The *h* parameter, taken as reaction coordinate, is defined in Methodology.

VI. SECOND HYDROGENATION

We have considered the possibilities for a second hydrogenation. Again, hydrogen can either bond to the nitrogen, leading to an imine (H–N=CH(CH_3)), or to the carbon, leading to a nitrene form (N–CH_2(CH_3)), doubly bonded with the metallic surface. The several adsorption modes we have considered for these two species are described in Scheme 2, and the relative energies obtained are reported in Table 4. Nitrene forms do not have a π system, so no η_2 mode is possible; they appear to be undoubtedly more stable than any of the adsorbed forms of imine and have already been reported (25). As in the case of imido-ethylidene, the stablest form of nitrene is η_1 in a hollow site. It is clear, since there is no π system, that the CN bond is perpendicular to the surface.

As before, several situations for the coadsorption of imido-ethylidene (η_1 hollow or η_2 fourfold) with atomic hydrogen have been considered. Three archetypal behaviors were encountered: first, cases where hydrogen is far from the adsorbed intermediate and hardly no interaction takes place; second, cases where hydrogen achieves a slightly positive overlap with either carbon or nitrogen, but the global result is a slight destabilization; and last, cases where hydrogen strongly destabilizes the imido-ethylidene. In all cases, the overlap population between H and C or N is larger with the carbon, indicating that hydrogen will prefer to bind with carbon than with nitrogen. For both modes of imido-ethylidene, we chose starting situations falling in case two. We have considered three different starting points for the second hydrogenation process and two possible products, resulting in four different competitive reaction steps. The energetic dependences with parameter h (see Methodology) for the four paths are plotted in Fig. 5. The paths leading to the hydrogenation on carbon are always favored whatever the starting mode (η_1 hollow or η_2 fourfold) and path (4) is clearly preferred, with an activation energy lower than 1 eV. Hence, the second hydrogenation occurs on carbon, leading to a nitrene species doubly bonded to the surface. Such a result has been observed on iron complexes (26). This is consistent with the polarity of the CN bond and the hydride aspect of the adsorbed hydrogen.

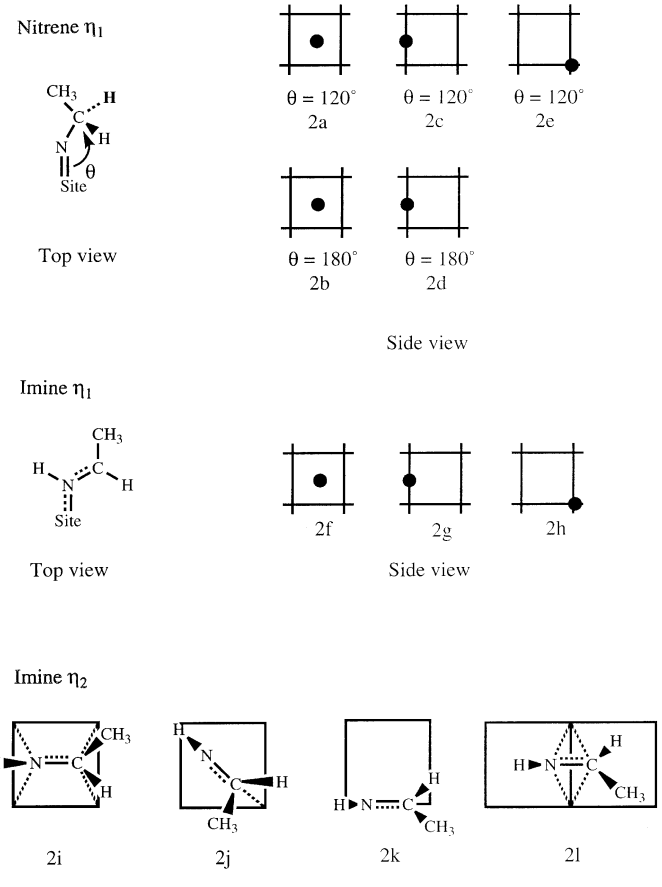

SCHEME 2. Adsorption geometries of the competitive second hydrogenation products of acetonitrile on Ni(100). See Table 4.

VII. REACTION PATHS TOWARD DIMERIZATION

As pointed out at the end of Section V, a coupling process between two adsorbed intermediates seems possible. This could account for the presence of by-products in the industrial reaction and is in agreement with interesting experimental observations. We will discuss now the factors that may influence the vicinal coadsorption of two nitriles. Among the possible adsorbed species, the η_1 hollow imido-ethylidene exhibits interesting radical properties, while other stable species on the surface (nitrile, η_2 fourfold imido-ethylidene) exhibit larger charge separations. Consequently, we have studied on a 110 atom cluster the possibilities of vicinal coadsorption of two η_1 hollow imido-ethylidenes. The coadsorption situations are depicted in Scheme 3 and the main characteristics are summarized in Table 5 (see "without chain"). In Scheme 3d, the two imido-ethylidenes coadsorb without loss of adsorption energy. We specially focused on the overlap population between the carbons noted C_1 and C_2 of the two imido-ethylidenes. Two kinds of situation appear: first, when C_1 and C_2 are far apart (more than 4 Å), the overlap population is zero or slightly negative; second, when the two imido-ethylidenes are adsorbed in two vicinal hollow sites (see Schemes 3a and 3b), there is a positive overlap population. These two situations, one noted *cis* because C_1 and C_2 are on the same side and the other noted *trans*, appear to be the best starting points for dimerization. They are also the less stable forms, which can be attributed to the steric hindrance of the two organic ends. We have studied the influence of the hybridization of C_1 and C_2 on the stability of the *cis* and *trans* intermediates (Schemes 3a and 3b). In both cases, for the optimal degree of hybridization, the stability of the whole is only 0.6 eV above the other forms we have considered, and

TABLE 4

Adsorption Energies of the Competitive Second Hydrogenation Products of Acetonitrile on Ni(100)

Intermediate type	Mode	Adsorption geometry (letters refer to Scheme 2)	Relative adsorption energy (eV)	Hybridization (η_2 modes)
Nitrene η_1	Hollow	2a	0.46	
		2b	0.00	
	Bridge	2c	0.86	
		2d	0.80	
	Top	2e	1.55	
Imine η_1	Hollow	2f	2.72	
	Bridge	2g	2.02	
	Top	2h	2.26	
Imine η_2	Fourfold	2i	1.62	1
	Di-σ diagonal	2j	2.16	1
	Di-σ	2k	2.04	1
	Di-σ $\perp$	2l	2.78	1

hence they appear as probable intermediates on the way to dimerization.

As we also specifically wanted to study the possibilities for cyclization of 1, 6-dinitrile hexane (adiponitrile), we performed calculations with this molecule in order to see how the hydrocarbon chain would effect the result we described with the two disjoined fragments. We have considered cases where the two nitrile ends of the molecule are monohydrogenated and simultaneously adsorbed on vicinal hollow sites. For each given coordination of the two ends, we used molecular modeling techniques (27) in order to minimize the energy of the chain. Once this energy was minimized, we kept the corresponding geometry for computations with the EH program. The results are also reported in Table 5 (see "with chain"). As *cis* forms are considered, the stability increases when the distance between the adsorption sites of the two ends decreases (compare Schemes 3k and 3i). For the *trans* forms, the opposite occurs: the stability is greater when the adsorption sites are not too close (compare Schemes 3j and 3l); this is related to the constraints imposed by the bridging hydrocarbon chain. Hence, we have two possible starting points (*cis* 3i or *trans* 3l) for

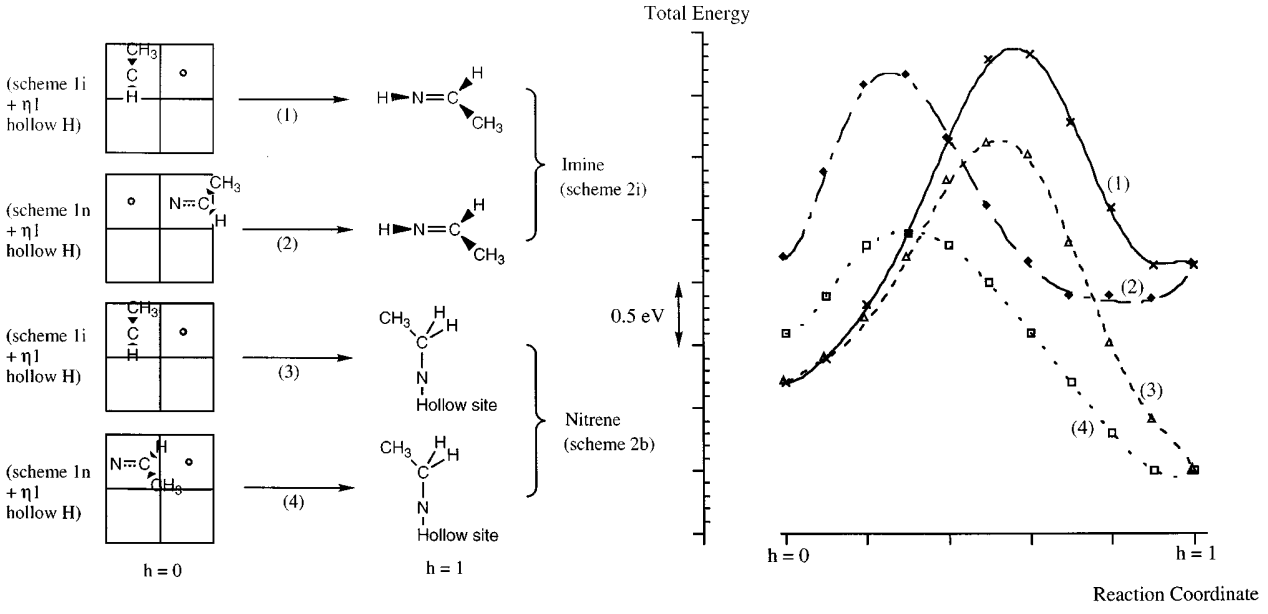

FIG. 5. Four of the most probable monohydrogenation steps of the adsorbed imido-ethylidene intermediate on Ni(100). The *h* parameter, taken as reaction coordinate, is defined in Methodology.

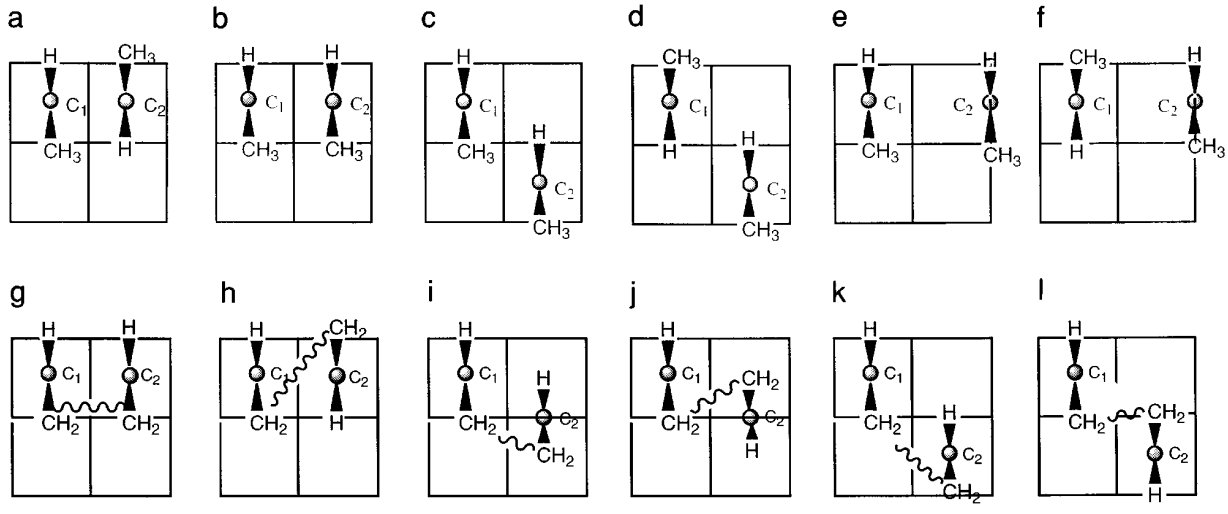

SCHEME 3.

coadsorption which, by comparison with Scheme 3d, correspond to hardly no energy loss. We therefore predict the coexistence of the two, *cis* and *trans*, cyclized products: 1,2-diamino-cyclohexane.

As for the previous reaction steps, we have studied the comparative stabilities of the possible forms of the dimer product. The results are sumarized in Table 6 and the corresponding geometries are described in Scheme 4. Again, we have performed calculations with and without the C_4 chain. The conclusions are that the most favorable products are when the two organic ends are adsorbed on next hollow sites with the NCCN plane perpendicular to the surface, and that the best *trans* adsorbed dimer is more stable than the *cis* in the case without the chain and, in contrast, less stable with the chain.

TABLE 5

Vicinal Coadsorption of Two η_1 Hollow Imido-Ethylidene Species

Model	Geometry (see Scheme 3)	Overlap pop. (C_1, C_2)	Distance (C_1, C_2) (Å)	ΔE (eV)
	3a	0.057	2.49	1.02 (0.66)[a]
	3b	0.063	2.49	3.30 (0.79)[a]
Without	3c	−0.003	3.52	0.59
chain	3d	0.000	3.52	0.00
	3e	−0.001	3.73	0.27
	3f	0.000	3.73	0.23
	3g	0.051	2.49	0.87
	3h	0.033	2.49	2.38
With chain	3i	0.003	2.78	0.11
	3j	−0.008	2.78	0.57
	3k	−0.002	3.52	0.46
	3l	−0.004	3.52	0.00

Note. Half of the cases involve a bridging hydrocarbon chain.

[a] The values in parentheses are obtained with the hybridization of the two carbons (see text).

We have studied the two dimerization process (*cis* → *cis* and *trans* → *trans*). As before, C–C distance, carbon hybridization, and site-N–C angle have been simultaneously varied by introducing a linear parameter *h*. The two energy

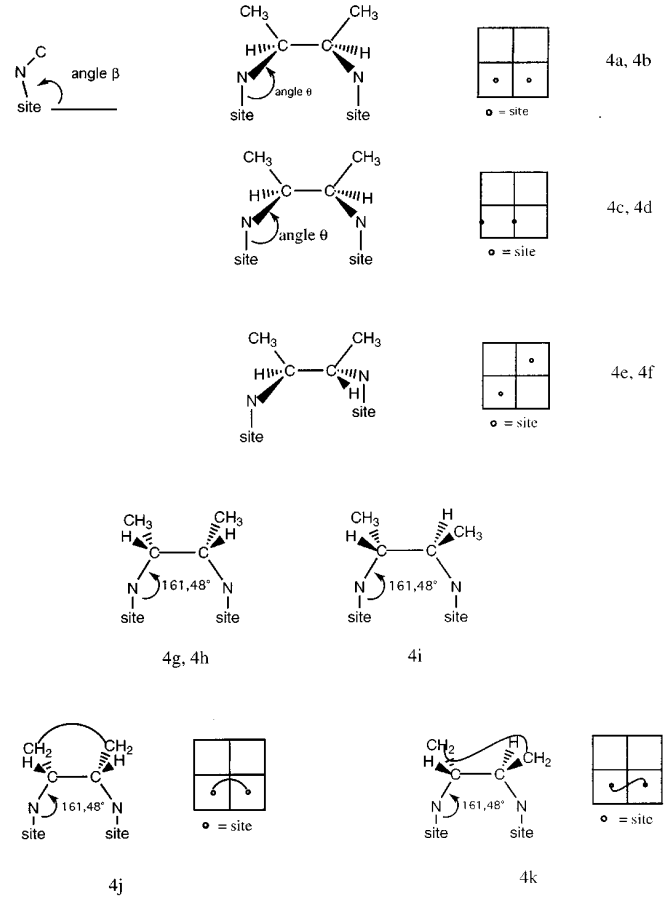

SCHEME 4.

TABLE 6

Energetic Characteristics of Several Possible Geometries for Dimers Diadsorbed on Ni[100]

Type	Model	Geometry (Scheme 4)	Site Ni_1	Site Ni_2	Angles (°)	ΔE (eV)
		4a	Hollow	Hollow	$\theta = 160°, \beta = 90°$	0.47
		4b	Hollow	Hollow	$\theta = 140°, \beta = 100°$	0.82
		4c	Bridge	Bridge	$\theta = 160°, \beta = 90°$	1.91
	Without chain	4d	Bridge	Bridge	$\theta = 140°, \beta = 100°$	2.42
		4e	Bridge	Bridge	$\theta = 120°, \beta = 90°$	4.14
		4f	Hollow	Hollow	$\theta = 120°, \beta = 90°$	2.21
		4g	Hollow	Hollow	$\theta = 161.8°, \beta = 90°$	0.44
		4h	Bridge	Bridge	$\theta = 161.8°, \beta = 90°$	1.88
		4i	Hollow	Hollow	$\theta = 161.8°, \beta = 90°$	0.00
	With chain	4j	Hollow	Hollow	$\theta = 161.8°, \beta = 90°$	0.00
		4k	Hollow	Hollow	$\theta = 161.8°, \beta = 90°$	1.14

profiles are given in Fig. 6. From the nonhybridized 3a and 3b situations, the two processes are spontaneous. This means that as soon as the two imidoethylidenes are adsorbed on vicinal hollow sites, dimerization occurs. This process can be decomposed as follows. The starting points are situations where the two molecules are adsorbed in two nonadjacent hollow sites (either in *cis* or *trans* position). Then, passing through 3e and 3f (0.27 eV and 0.23 eV above, respectively), one arrives at hybridized 3b and 3a (0.79 eV and 0.66 eV above, respectively), which represent the transition states since we have just seen that the reaction then evolves smoothly to the final products.

The reaction paths have not been calculated for the cases where the chain is taken into account, because each point requires the computation of the best conformation for the chain. However, following previous results, we can assume that situations 3l and 3i can lead to cyclization with a small activation energy (in the range 0.7–0.8 eV).

In conclusion, the three reactions considered in this work, namely monohydrogenation, dihydrogenation, and dimerization (cyclization), have activation energies of the same magnitude. Hence, the key parameter for the existence of this dimerization path competing with the total hydrogenation is the possibility for 1, 6-dinitrile-hexane (adiponitrile) to have its two ends simultaneously adsorbed on next hollow sites and at the same imido-ethylidene state of hydrogenation: if this is achieved, dimerization may occur.

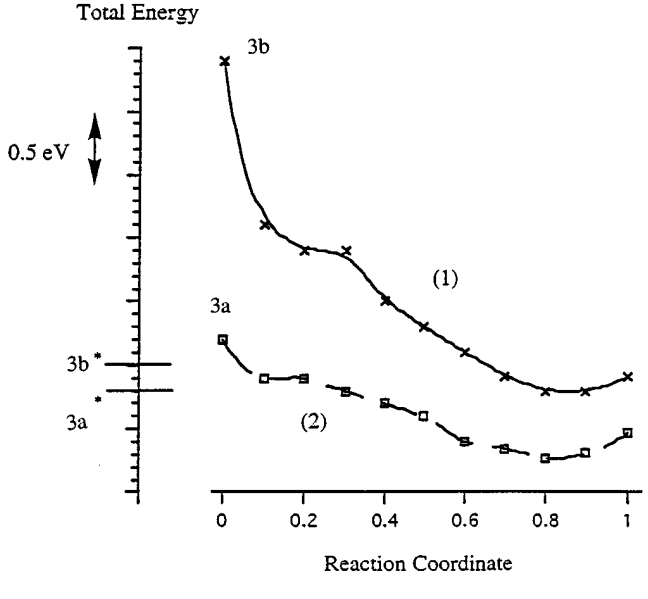

FIG. 6. Energy profiles on the competitive *cis* (1) and *trans* (2) dimerization processes. The reaction coordinate is defined in Methodology (see also text). (*) After hybridization of C_1 and C_2.

VIII. CONCLUSION

The present study offers a theoretical overview on the whole hydrogenation process of nitriles on nickel. Although it is incomplete, since the whole process has only been studied on Ni(100) and with one type of dimers (other products of coupling processes have also been reported (28)), we may conclude that the tendencies observed are valid for Raney nickel, which presents several different planes for adsorption, especially (100). We have shown that the first and second hydrogenations both take place on carbon leading to species strongly adsorbed on the surface with an activation energy of about 1 eV. Finally, we have to address the question of the parameters which could influence the competition between full hydrogenation and dimerization in the case of 1,6-dinitrile. The question is immediately related to the possibilities of vicinal η_1 coadsorption of the two organic ends. The factors that favor this are large clean faces of the catalyst, and the length (C_6) of the hydrocarbon chain which is optimal for adsorption with a N–N distance of 2.49 Å, due to epitaxy on the hollow sites. The factors that may hinder the formation of cyclized products are a high pressure of

hydrogen that may cover the surface, a stepped and uneven catalyst surface (as is the case with finely divided Raney nickel), the presence on the catalyst surface of doping compounds, and structural promoters or poisons. Another way to hinder cyclization is to have the imido-ethylidene adsorbed in a η_2 manner since these situations do not allow dimerization; this could been achieved by the use of coadsorbates or of metallic salts (see (29)). The industrial conditions make it clear why the desired full hydrogenation product is overwhelmingly dominant; we show here how to favor further this situation, by using a well-covered catalyst, either in hydrogen or in compounds that may spread evenly on the surface occupying one every two sites. We also predict that hydrogenation of dinitriles with shorter or longer hydrocarbon chain in between would yield less cyclized products of this kind. An interesting sequel to this work would involve similar studies on Ni(111) and Ni(110), and would aim at taking into account reconstruction phenomena and the existence of steps or kinks, bringing our surface model closer to experimental reality.

ACKNOWLEDGMENTS

This work has been supported by Rhône-Poulenc. Dr. J. Jenck and Dr. M. Joucla, from Rhône-Poulenc Research Center in Décines (France), are acknowledged for useful comments and discussions. The Institut du Développement et des Ressources en Informatique Scientifique is also acknowledged for a generous allocation of computer time.

REFERENCES

1. Bigot, B., Delbecq, F., and Peuch, V.-H., *Langmuir* **11**, 3828 (1995).
2. (a) Sautet, P., and Paul, J. F., *Catal. Lett.* **9**, 245 (1991); (b) Delbecq, F., and Sautet, P., *Catal. Lett.* **28**, 89 (1994).
3. (a) Delbecq, F., and Sautet, P., *Langmuir* **9**, 197 (1993); (b) *Surf. Sci.* **295**, 353 (1993); (c) *J. Catal.* **152**, 217 (1995).
4. (a) Fassaert, D. J. M., and van der Avoid, A., *Surf. Sci.* **55**, 291 (1976); (b) *Surf. Sci.* **55**, 313 (1976).
5. Yang, H., and Whitten, J. L., *J. Chem. Phys.* **89** (8), 5329 (1988).
6. Nørskov, J. K., *Phys. Rev. Lett.* **48**, 1620 (1982).
7. Gavin, R. M., Reutt, J., and Muetterties, E. L., *Proc. Natl. Acad. Sci. USA* **78**, 3981 (1981).
8. Ferullo, R. M., and Castellani, N. J., *J. Al. Com.* **191**, 173 (1993).
9. (a) Christmann, K., *Molec. Phys.* **66**, 1 (1989); (b) Christmann, K., Schober, O., Ertl, G., and Neumann, M., *J. Chem. Phys.* **60**, 4528 (1974); (c) Christmann, K., Behm, R. J., Ertl, G., *J. Chem. Phys.* **70**, 4168, (1979).
10. Parschau, G., Burg, B., and Rieder, K. H., *Surf. Sci. Lett.* **293**, 830 (1993).
11. Yacaman, M. J., and Dominguez, E. J. M., *J. Catal.* **64**, 213 (1980).
12. Szanyi, J., Kuhn, W. K., and Goodman, D. W., *J. Vac. Sci. Technol. A* **11**, 1969 (1993).
13. Mays, M. J., Prest, D. W., and Raithby, P. R., *J. Chem. Soc. Chem. Commun.* 171 (1980).
14. Dawoodi, Z., Mays, M. J., and Raithby, P. R., *J. Organomet. Chem.* **219**, 85 (1981).
15. He, Z., Neidebecker, D., Lugan, N., and Mathieu, R., *Organometallics* **11**, 817 (1992).
16. Garcia Alonsa, F. J., Sanz, M. G., Riera, V., Anillo Abil, A., Tiripicchio, A., and Ugozzoli, F., *Organometallics* **11**, 801 (1992).
17. Rehbaum, F., and Thiel, K. H., *J. Organomet. Chem.* **410**, 327 (1991).
18. Bellachioma, G., Gardaci, G., and Zanazzi, P., *Inorg. Chem.* **26**, 84 (1987).
19. Roskamp, E. J., and Pedersen, S. F., *J. Am. Chem. Soc.* **109**, 3152 (1987).
20. Hochard, F., Jobic, H., Massardier, J., and Renouprez, A. J., *J. Mol. Catal.* **95**, 165 (1995).
21. Sautet, P., and Paul, J.-F., submitted for publication.
22. Verhaak, M. J. F. M., Van Dillen, A. J., and Geus, J. W., *J. Catal.* **143**, 187 (1993).
23. Gardin, D. E., and Somorjai, G. A., *J. Phys. Chem.* **96**, 9424 (1992).
24. Ditlevsen, P. D., Gardin, D. E., van Hove, M. A., and Somorjai, G. A., *Langmuir* **9**, 1500 (1993).
25. Bock, H., and Breuer, O., *Angew. Chem. Int. Engl. Ed.* **7**, 461 (1987).
26. Andrews, M. A., and Kaesz, H. D., *J. Am. Chem. Soc.* **101**, 7255 (1979).
27. Lahana, R., Molecular Advanced Design v.2.0, © Pierre Fabre Medicaments (1987, 1991).
28. Marion, Ph., Grenouillet, P., Jenck, J., and Joucla, M., *Stud. Surf. Sci. Catal.* **59**, 329 (1991).
29. (a) Medina, F., Salagre, P., Sueiras, J. E., and Fierro, J. L. G., *J. Mol. Catal.* **81**, 363 (1993); (b) *J. Mol. Catal.* **81**, 387 (1993).